Entangled State Reconstruction of an Electron in the Penning Trap

Mauro Fortunato, Michol Massini, Stefano Mancini, and Paolo Tombesi

INFM and Dipartimento di Matematica e Fisica, Università di Camerino,
Via Madonna delle Carceri I-62032 Camerino

Reprint requests to Dr. M. F. E-mail: mauro@camcat.unicam.it

Z. Naturforsch. **56 a,** 145–151 (2001); received February 15, 2001

Presented at the 3rd Workshop on Mysteries, Puzzles and Paradoxes in Quantum Mechanics, Gargnano, Italy, September 17 - 23, 2000.

We apply a tomographic method we have recently proposed to the reconstruction of the full entangled quantum state for the cyclotron and spin degrees of freedom of a trapped electron. Our numerical simulations show that the entangled state is accurately reconstructed. – Pacs: 03.65.-w, 03.65.Bz, 42.50.Vk, 42.50.Dv

Key words: State Reconstruction; Entanglement; Trapped Electron; Penning Trap; Quantum Information.

1. Introduction

Entanglement [1] is one of the essential and most puzzling features of quantum mechanics. It is also the basic ingredient and resource of quantum information processing: quantum teleportation [2, 3], quantum dense coding [4], quantum cryptography [5], and quantum computation [6] are just a few examples of the possibilities offered by sharing quantum entanglement. Recently, for example, it has been made possible to entangle four trapped ions [7].

The quantum system we want to study here is a single electron trapped in a Penning trap [8]. This system allows the measurement of fundamental physical constants with striking accuracy and is reasonably free of decoherence and dissipation [9]. As a consequence, the determination (or the *reconstruction* [10]) of the entangled quantum state of the trapped electron is a decisive issue, especially in the light of the fact that such a system has been already proposed as a candidate for quantum information processing [11].

In this paper we propose to reconstruct the full *entangled* state (combined cyclotron and spin state) of an electron in a Penning trap by using a modified version of quantum state tomography. Previous proposals [12] need the *a priori* knowledge of the spin state and therefore are not able to deal with entangled states. Our method, on the contrary, can measure the full (entangled) pure state of the two relevant degrees of freedom of the electron. In order to reach this scope, our method takes advantage of the magnetic bottle configuration to perform simultaneous measurements of the cyclotron excitation and of the z component of the spin as a function of the phase of an applied driving electromagnetic field. The complete structure of the cyclotron-spin quantum state is then obtained with the help of a tomographic reconstruction from the measured data.

The present paper is organized as follows: In Sect. 2 we describe the basic physics of an electron trapped in a Penning trap, while in Sect. 3 we present our reconstruction procedure. In Sects 4 and 5 we concentrate on the measurement of the spin and on the tomographic reconstruction of the cyclotron states, respectively. We finally discuss the results of our numerical simulations in Section 6.

2. The System

Let us consider the motion of an electron trapped by the combination of a homogeneous magnetic field $\boldsymbol{B}_0$ along the positive z axis and an electrostatic quadrupole potential in the xy plane, which is known as a *Penning trap* [8]. The corresponding Hamiltonian can be written as

$$\hat{H} = \frac{1}{2m}\left[\boldsymbol{p} - \frac{q}{c}\boldsymbol{A}\right]^2 + \frac{qV_0}{2d^2}\left(\hat{z}^2 - \frac{\hat{x}^2 + \hat{y}^2}{2}\right), \quad (1)$$

0932–0784 / 01 / 0100–0145 $ 06.00

where $\boldsymbol{A} = (B_0 y/2, -B_0 x/2, 0)$ is the vector potential, c is the speed of light, d characterizes the dimensions of the trap, V_0 is the electrostatic potential applied to its electrodes, and q the electron charge.

The spatial part of the electronic wave function consists of three degrees of freedom, but neglecting the slow magnetron motion (whose characteristic frequency lies in the kHz region), here we only consider the axial and cyclotron motions, which are two harmonic oscillators radiating in the MHz and GHz regions, respectively. The spin dynamics results from the interaction between the magnetic moment of the electron and the magnetic field, so that the total quantum Hamiltonian is

$$\hat{H}_{\rm tot} = \hbar\omega_z(\hat{a}_z^\dagger \hat{a}_z + 1/2) + \hbar\omega_{\rm c}(\hat{a}_{\rm c}^\dagger \hat{a}_{\rm c} + 1/2) + \frac{\hbar\omega_{\rm s} s}{2}\hat{\sigma}_z. \quad (2)$$

In this expression we have introduced the lowering operator for the cyclotron motion

$$\hat{a}_{\rm c} = \frac{1}{2}\Big[\frac{1}{2\beta\hbar}(\hat{p}_x - i\hat{p}_y) - i\beta(\hat{x} - i\hat{y})\Big], \quad (3)$$

where $\beta = m\omega_{\rm c}/2\hbar$ and $\omega_{\rm c} = qB_0/mc$ is the resonance frequency associated with the cyclotron oscillation. For the axial motion we have

$$\hat{a}_z = \Big(\frac{m\omega_z}{2\hbar}\Big)^{1/2}\hat{z} + i\Big(\frac{1}{2m\hbar\omega_z}\Big)^{1/2}\hat{p}_z, \quad (4)$$

where $\omega_z^2 = qV_0/md^2$. In the last term of (2), $\hat{\sigma}_z$ is the Pauli spin matrix and $\omega_{\rm s} = (g/2)\omega_{\rm c}$.

The obtained Hamiltonian (2) is then made of three independent terms. Even though the only physical observable experimentally detectable is the axial momentum $\hat{p}_z$, in the following both the cyclotron and spin states will be reconstructed. Considering the eigenstates of $\hat{\sigma}_z$

$$|\uparrow\rangle_{\rm s} = \begin{pmatrix} 1 \\ 0 \end{pmatrix}, \; |\downarrow\rangle_{\rm s} = \begin{pmatrix} 0 \\ 1 \end{pmatrix}, \quad (5)$$

where the subscript s stands for spin, we can write the most general pure state of the trapped electron in the form

$$|\Psi\rangle_{\rm cs} = c_1|\psi_1\rangle_{\rm c}|\uparrow\rangle_{\rm s} + c_2|\psi_2\rangle_{\rm c}|\downarrow\rangle_{\rm s}, \quad (6)$$

where the subscript c stands for cyclotron, $|\psi_1\rangle_{\rm c}$ and $|\psi_2\rangle_{\rm c}$ being two unknown cyclotron states. The complex coefficients c_1 and c_2, satisfying the normalization condition $|c_1|^2 + |c_2|^2 = 1$, are also to be determined.

The electronic state (6) is an *entangled state* between the spin and cyclotronic degrees of freedom. Introducing the total density operator $\hat{R}_{\rm cs} = |\Psi\rangle_{\rm cs}\langle\Psi|$, we can express the corresponding total density matrix $R_{\rm cs}$ in the basis of the eigenstates (5) of $\hat{\sigma}_z$ in the form

$$R_{\rm cs} = \begin{pmatrix} |c_1|^2|\psi_1\rangle_{\rm c}\langle\psi_1| & c_1c_2^*|\psi_1\rangle_{\rm c}\langle\psi_2| \\ c_2c_1^*|\psi_2\rangle_{\rm c}\langle\psi_1| & |c_2|^2|\psi_2\rangle_{\rm c}\langle\psi_2| \end{pmatrix}, \quad (7)$$

whose elements are operators. Its diagonal elements represent the possible cyclotron states, while the off-diagonal ones are the quantum coherences and contain information about the quantum interference effects due to the entanglement between the spin and cyclotron degrees of freedom.

It is also possible to give a phase-space description of the complete quantum state of the trapped electron by introducing the Wigner-function matrix [13] whose elements are given by

$$W_{ij}(\alpha) = \langle\hat{\delta}_{ij}(\alpha - \hat{a})\rangle = {\rm Tr}[\hat{R}_{\rm cs}\hat{\delta}_{ij}(\alpha - \hat{a})], \quad (8)$$

where $i, j = 1, 2$ and $\hat{\delta}_{ij}(\alpha - \hat{a})$ is an operator in the product Hilbert space $\mathcal{H} = \mathcal{H}_{\rm cyc} \otimes \mathcal{H}_{\rm spin}$ defined as

$$\hat{\delta}_{ij}(\alpha - \hat{a}) = |i\rangle\langle j|\hat{\delta}(\alpha - \hat{a}). \quad (9)$$

In this expression the operator-valued delta function $\hat{\delta}(\alpha - \hat{a})$ is the Fourier transform of the displacement operator $\hat{D}(\alpha) = \exp(\alpha\hat{a}^\dagger - \alpha^*\hat{a})$.

3. Electron Tomography

The basic idea of our reconstruction procedure is very simple: Adding a particular inhomogeneous magnetic field – known as the "magnetic bottle" field [8] – to that already present in the trap, it is possible to perform a simultaneous measurement of both the spin and the cyclotronic excitation numbers. Repeated measurements of this type allow us to recover the probability amplitudes of the two possible spin states and the cyclotron probability distribution $P(n_{\rm c})$ in the Fock basis. The reconstruction of the cyclotron density matrices $\rho_{ii} = |\psi_i\rangle_{\rm c}\langle\psi_i|$ $(i = 1, 2)$ in the Fock basis is then possible by employing a technique similar to the Photon Number Tomography (PNT) [12, 14] which exploits a phase-sensitive

reference field that displaces in the phase space the particular state one wants to reconstruct [15].

In close analogy with the procedure described in [8, 14], the coupling between the different degrees of freedom in (2) is obtained by modifying the vector potential with the addition of the magnetic bottle field [8], so that $\boldsymbol{A}$ takes the form

$$\boldsymbol{A} = \frac{1}{2}\Big[- B_0\hat{y} - b\Big(\hat{y}\hat{z}^2 - \frac{\hat{y}^3}{3}\Big), \\ B_0\hat{x} + b\Big(\hat{x}\hat{z}^2 - \frac{\hat{x}^3}{3}\Big), 0\Big]. \tag{10}$$

Such a vector potential gives rise to an interaction term in the total Hamiltonian,

$$\hat{H}_{\rm int} = \hbar\kappa\Big[\Big(\hat{a}_{\rm c}^{\dagger}\hat{a}_{\rm c} + \frac{1}{2}\Big) + \frac{g}{2}\frac{\hat{\sigma}_z}{2}\Big]\hat{z}^2, \tag{11}$$

where the coupling constant $\kappa = qb/mc$ is directly related to the strength b of the magnetic bottle field.

Equation (11) describes the fact that the axial angular frequency is affected both by the number of cyclotron excitations $\hat{n}_{\rm c} = \hat{a}_{\rm c}^{\dagger}\hat{a}_{\rm c}$ and by the eigenvalue of $\hat{\sigma}_z$. In terms of the lowering operator $\hat{a}_z$ for the axial degree of freedom, the Hamiltonian that describes the interaction among the axial, cyclotron, and spin motions can be written as

$$\hat{H}_{\rm czs} = \hbar\omega_z\Big(\hat{a}_z^{\dagger}\hat{a}_z + \frac{1}{2}\Big)\frac{\hat{\Omega}_z^2}{\omega_z^2}, \tag{12}$$

where the operator frequency $\hat{\Omega}_z$ is given by

$$\hat{\Omega}_z^2 = \omega_z^2 + \frac{\hbar\kappa}{m}\Big[\Big(\hat{a}_{\rm c}^{\dagger}\hat{a}_{\rm c} + \frac{1}{2}\Big) + \frac{g}{4}\hat{\sigma}_z\Big]. \tag{13}$$

The operator $\hat{\Omega}_z$ is the modified axial frequency which can be experimentally measured [8] after the application of the inhomogeneous magnetic bottle field. What is actually measured is an electric current (which is proportional to $\hat{p}_z$) that gives the axial frequency shift $\hat{\Omega}_z^2$ [8]. One immediately sees that the spectrum of $\hat{\Omega}_z$ is discrete: Since the electron g factor is slightly (but measurably [8]) different from 2, $\hat{\Omega}_z$ assumes a different value for every pair of eigenvalues of $\hat{n}_{\rm c}$ and $\hat{\sigma}_z$.

4. Spin Measurements

If one can perform a large set of measurements of $\hat{\Omega}_z$ in such a way that before each measurement the state $|\Psi\rangle$ is always prepared in the same way, it is possible to recover the probabilities $P(\uparrow)$ and $P(\downarrow)$ of the two possible eigenvalues of $\hat{\sigma}_z$, namely $|c_1|$ and $|c_2|$. Recalling (6), we have

$$P(\uparrow) = {\rm Tr}_{\rm cyc}[\langle\uparrow|\Psi\rangle_{cs}\langle\Psi|\uparrow\rangle] = |c_1|^2, \tag{14}$$

$$P(\downarrow) = {\rm Tr}_{\rm cyc}[\langle\downarrow|\Psi\rangle_{cs}\langle\Psi|\downarrow\rangle] = |c_2|^2 = 1 - P(\uparrow). \tag{15}$$

However, this kind of measurement does not allow to retrieve the relative phase θ between the complex coefficients c_1 and c_2 in the superposition (6). We can then add a time-dependent magnetic field $\boldsymbol{b}_0(t)$ oscillating in the xy plane perpendicular to the trap axis [8], i. e.

$$\boldsymbol{b}_0(t) = b_0\cos(\omega t)\hat{\boldsymbol{x}} + b_0\sin(\omega t)\hat{\boldsymbol{y}}. \tag{16}$$

The resulting interaction Hamiltonian in the interaction picture is

$$\hat{H}_{\rm rot}^{\rm I}(t) = \exp\Big[\frac{i}{\hbar}\hat{H}_0 t\Big]\hat{H}_{\rm rot}(t)\exp\Big[-\frac{i}{\hbar}\hat{H}_0 t\Big] \\ = \frac{\hbar}{2}[(\omega_{\rm s} - \omega)\hat{\sigma}_z + \omega_R\hat{\sigma}_x], \tag{17}$$

where

$$\hat{H}_0 = \frac{\hbar\omega}{2}\hat{\sigma}_z\,, \tag{18}$$

and

$$\hat{H}_{\rm rot}(t) = \frac{\hbar}{2}\big[(\omega_{\rm s} - \omega)\hat{\sigma}_z + \omega_{\rm R}\big(\hat{\sigma}_x\cos(\omega t) \\ + \hat{\sigma}_y\sin(\omega t)\big)\big]. \tag{19}$$

In the above equations, $\hat{H}_{\rm rot}(t)$ is the interaction Hamiltonian in a frame rotating with the driving frequency ω, while $\omega_R = gqb_0/2mc$ is the Rabi frequency.

The evolution of the state (6), subjected to the Hamiltonian (17) in the resonant case $\omega = \omega_{\rm s}$, yields the state

$$|\Psi(\bar{t})\rangle_{\rm cs} = \exp\Big[-\frac{i}{\hbar}\hat{H}_{\rm rot}^{\rm I}(t)\bar{t}\Big]|\Psi\rangle_{\rm cs} \\ = \frac{\sqrt{2}}{2}\big[(c_1|\psi_1\rangle_{\rm c} - ic_2|\psi_2\rangle_{\rm c})|\uparrow\rangle_{\rm s} \\ + (-ic_1|\psi_1\rangle_{\rm c} + c_2|\psi_2\rangle_{\rm c})|\downarrow\rangle_{\rm s}\big], \tag{20}$$

obtained applying the driving field (16) for a time $\bar{t} = \pi/2\omega_R$. We can now repeat the spin measurements just as we have described above in the case of the *unknown* initial state $|\Psi\rangle$: Soon after $\boldsymbol{b}_0(t)$ is switched off, the magnetic bottle field is applied again and the spin measurement is performed. Repeating this procedure over and over again (with the same unknown initial state) for a large number of times, it is possible to recover the probabilities $\bar{P}(\uparrow)$ and $\bar{P}(\downarrow)$ of the two spin eigenvalues for the state $|\Psi(\bar{t})\rangle_{cs}$ of (20). Without loss of generality, we can assume $c_1 \in R$, $c_2 = |c_2|e^{i\theta}$, and ${}_c\langle\psi_1|\psi_2\rangle_c = re^{i\beta}$, which yields

$$\bar{P}(\uparrow) = \frac{1}{2}\left[1 + 2r|c_1||c_2|\sin(\theta+\beta)\right], \tag{21}$$

$$\bar{P}(\downarrow) = \frac{1}{2}\left[1 - 2r|c_1||c_2|\sin(\theta+\beta)\right]. \tag{22}$$

It is important to note that the probabilities $\bar{P}(\uparrow)$ and $\bar{P}(\downarrow)$ can be experimentally sampled and that the modulus r and the phase β of the scalar product $\langle\psi_1|\psi_2\rangle$ can be derived from the reconstruction of the cyclotron density matrices ρ_{11} and ρ_{22}, as we shall explain in the next section. Thus we are able to find the relative phase θ by simply inverting one of the two Eqs. (21, 22), e. g.

$$\theta = \arcsin\left[\frac{2\bar{P}(\uparrow) - 1}{2r|c_1||c_2|}\right] - \beta\,. \tag{23}$$

The resulting π ambiguity in the arcsin function on the right hand side of (23) can be eliminated by choosing a second interaction time $\bar{t}'$ and repeating the procedure above.

5. The Cyclotron State

Let us consider again the state of (6): every time $\hat{\Omega}_z$ (and therefore $\hat{\sigma}_z$) is measured, the total wave function is projected onto $|\uparrow\rangle_s|n_c\rangle_c$ or $|\downarrow\rangle_s|n_c\rangle_c$, where $|n_c\rangle_c$ is a Fock state of the cyclotron. We then propose a tomographic reconstruction technique in which the state to be measured is combined with a reference field whose complex amplitude is externally varied (as it is usually done in optical homodyne tomography) in order to displace the *unknown* density operator in the phase space. In particular, we shall sample the cyclotron density matrix in the Fock basis by varying only the phase φ of the reference field, leaving its modulus $|\alpha|$ unaltered [12, 15, 16].

Following [12], immediately before the measurement of $\hat{\Omega}_z$ we apply to the trap electrodes a driving field generated by the vector potential

$$\boldsymbol{A} = \left(2\frac{mc}{\beta|q|}\mathrm{Im}[\epsilon e^{-i\omega_c t}], 2\frac{mc}{\beta|q|}\mathrm{Re}[\epsilon e^{-i\omega_c t}], 0\right), \tag{24}$$

where ϵ is the field amplitude, which gives rise to a Hamiltonian term of the form

$$\hat{H}_{\mathrm{drive}} = -i\hbar(\epsilon e^{-i\omega_c t}\hat{a}_c^\dagger - \epsilon^* e^{i\omega_c t}\hat{a}_c). \tag{25}$$

According to the Hamiltonian (25), the time evolution of the projected density operator $\hat{\rho}_{ii}$ $(i = 1, 2)$ may then be written in the cyclotron interaction picture as

$$\begin{aligned}\hat{\rho}_{ii}(\epsilon, t) &= \exp\left(\frac{i}{\hbar}\tilde{H}_{\mathrm{drive}}t\right)\hat{\rho}_{ii}(0)\exp\left(-\frac{i}{\hbar}\tilde{H}_{\mathrm{drive}}t\right)\\ &= \hat{D}^\dagger(\alpha)\hat{\rho}_{ii}(0)\hat{D}(\alpha),\end{aligned} \tag{26}$$

where we have defined the complex parameter $\alpha = \epsilon t$ (t being the interaction time) and $\tilde{H}_{\mathrm{drive}}$ is given by

$$\tilde{H}_{\mathrm{drive}} = -i\hbar(\epsilon\hat{a}_c^\dagger - \epsilon^*\hat{a}_c). \tag{27}$$

The right-hand side of (26) is then the desired displaced density operator, where the displacement parameter α is a function of both the strength ϵ of the driving field and the interaction time t. Thus we can interpret the quantity

$$\begin{aligned}P^{(i)}(n_c, \alpha) &= \mathrm{Tr}[\hat{\rho}_{ii}(\alpha)|n_c\rangle\langle n_c|]\\ &= \langle n_c|\hat{D}^\dagger(\alpha)\hat{\rho}_{ii}(0)\hat{D}(\alpha)|n_c\rangle\\ &= \langle n_c, \alpha|\hat{\rho}_{ii}(0)|n_c, \alpha\rangle\end{aligned} \tag{28}$$

as the probability of finding the cyclotron state $|\psi_i\rangle$ with an excitation number n_c after the application of the driving field of amplitude ϵ for a time t. Fixing a particular value of α and measuring $\hat{n}_c$, it is then possible to recover the probability distribution (28) by performing many identical experiments.

Expanding the density operator $\hat{\rho}_{ii}$ in the Fock basis and defining N_c as an appropriate estimate of the maximum number of cyclotronic excitations (cut-off), we have

$$P^{(i)}(n_c, \alpha) = \sum_{k,m=0}^{N_c}\langle n_c, \alpha|k\rangle\langle k|\hat{\rho}_{ii}|m\rangle\langle m|n_c, \alpha\rangle. \tag{29}$$

The projection of the displaced number state $|n_c, \alpha\rangle$ onto the Fock state $|m\rangle$ can be obtained as

$$\langle m|n,\alpha\rangle = \langle m|\hat{D}(\alpha)|n\rangle$$

$$= e^{-|\alpha|^2}\sqrt{\frac{\nu!}{\mu!}}|\alpha|^{\mu-\nu}\exp\{i(m-n)[\varphi-\pi\theta(n-m)]\}$$

$$\cdot\, L_\nu^{\mu-\nu}(|\alpha|^2), \tag{30}$$

where $\theta(x)$ is the Heaviside function, L_ν^μ the associated Laguerre polynomial, and $\mu = \max\{m,n\}$, $\nu = \min\{m,n\}$. Inserting (30) into (29), we get

$$P^{(i)}(n,\alpha) = e^{-|\alpha|^2}\sum_{k,m=0}^{N_c}\sqrt{\frac{\nu!\bar{\nu}!}{\mu!\bar{\mu}!}}|\alpha|^{\mu+\bar{\mu}-\nu-\bar{\nu}}$$

$$\cdot\, L_\nu^{\mu-\nu}(|\alpha|^2)e^{i(m-k)\varphi-\pi[(m-n)\theta(n-m)-(k-n)\theta(n-k)]}$$

$$\cdot\, L_{\bar{\nu}}^{\bar{\mu}-\bar{\nu}}(|\alpha|^2)\langle k|\hat{\rho}_{ii}|m\rangle, \tag{31}$$

where $\bar{\mu} = \max\{k,n\}$ and $\bar{\nu} = \min\{k,n\}$.

Let us now consider, for a given value of $|\alpha|$, $P^{(i)}(n,\alpha)$ as a function of φ and calculate the coefficients of the Fourier expansion

$$P^{(s,i)}(n,|\alpha|) = \frac{1}{2\pi}\int_0^{2\pi} \mathrm{d}\varphi\, P^{(i)}(n,\alpha)e^{i\varphi} \tag{32}$$

for $s = 0,1,2,\ldots$. Combining (31) and (32), we get

$$P^{(s,i)}(n,|\alpha|) = \sum_{m=0}^{N_c-s} G_{n,m}^{(s)}(|\alpha|)\langle m+s|\hat{\rho}_{ii}|m\rangle, \tag{33}$$

where we have introduced the matrices

$$G_{n,m}^{(s)}(|\alpha|) = e^{i\pi[(s+m-n)\theta(n-s-m)-(m-n)\theta(n-m)]}e^{-|\alpha|^2}$$

$$\cdot\sqrt{\frac{\nu!\bar{\nu}!}{\mu!\bar{\mu}!}}|\alpha|^{\mu+\bar{\mu}-\nu-\bar{\nu}}L_\nu^{\mu-\nu}(|\alpha|^2)L_{\bar{\nu}}^{\bar{\mu}-\bar{\nu}}(|\alpha|^2), \tag{34}$$

with $\bar{\mu} = \max\{m+s,n\}$ and $\bar{\nu} = \min\{m+s,n\}$.

We may now note that, if the distribution $P^{(i)}(n,\alpha)$ is measured for $n \in [0,N]$ with $N \geq N_c$, then (33) represents for each value of s a system of $N+1$ linear equations between the $N+1$ measured quantities and the $N_c + 1 - s$ unknown density matrix elements. Therefore, in order to obtain the latter, we only have to invert the system

$$\langle m+s|\hat{\rho}_{ii}|m\rangle = \sum_{n=0}^{N} M_{m,n}^{(s)}(|\alpha|)P^{(s,i)}(n,|\alpha|), \tag{35}$$

where the matrices M are given by $M = (G^TG)^{-1}G^T$. It is possible to see that these matrices satisfy the relation

$$\sum_{n=0}^{N} M_{m',n}^{(s)}(|\alpha|)G_{n,m}^{(s)}(|\alpha|) = \delta_{m',m}\,, \tag{36}$$

for $m,m' = 0,1,\ldots,N_c - s,\ldots$, which means that from the exact probabilities satisfying (33) the correct density matrix elements are obtained. Furthermore, combining (32) and (35), we find

$$\langle m+s|\hat{\rho}_{ii}|m\rangle$$

$$= \frac{1}{2}\sum_{n=0}^{N}\int_0^{2\pi}\mathrm{d}\varphi\, M_{m,n}^{(s)}(|\alpha|)e^{is\varphi}P^{(i)}(n,\alpha), \tag{37}$$

which may be regarded as the formula for the direct sampling of the cyclotron density matrix.

We now only have to reconstruct the off-diagonal parts of the total density matrix (7), *i.e.* $\hat{\rho}_{12} = \hat{\rho}_{21}^\dagger = |\psi_1\rangle\langle\psi_2|$. This can easily be done using the recursion relation

$$(\rho_{12})_{n,m} = \frac{\sum_{i=0}^{N}(\rho_{11})_{n,i}(\rho_{22})_{i,m}}{\langle\psi_1|\psi_2\rangle}. \tag{38}$$

6. Results and Discussion

In this section we show the results of numerical Monte-Carlo simulations of the method presented above. In particular, we shall present, as an example of application of the above method, the simulated tomographic reconstruction of an entangled electronic state of the type

$$|\Psi\rangle_{cs} = c_1|0\rangle_c|\uparrow\rangle_s + c_2e^{i\theta}|1\rangle_c|\downarrow\rangle_s, \tag{39}$$

in which c_1, c_2, and θ are real parameters. This state is particularly relevant for quantum information processing. We shall display the results of our simulations in terms of the Wigner-function matrix [13] of (8).

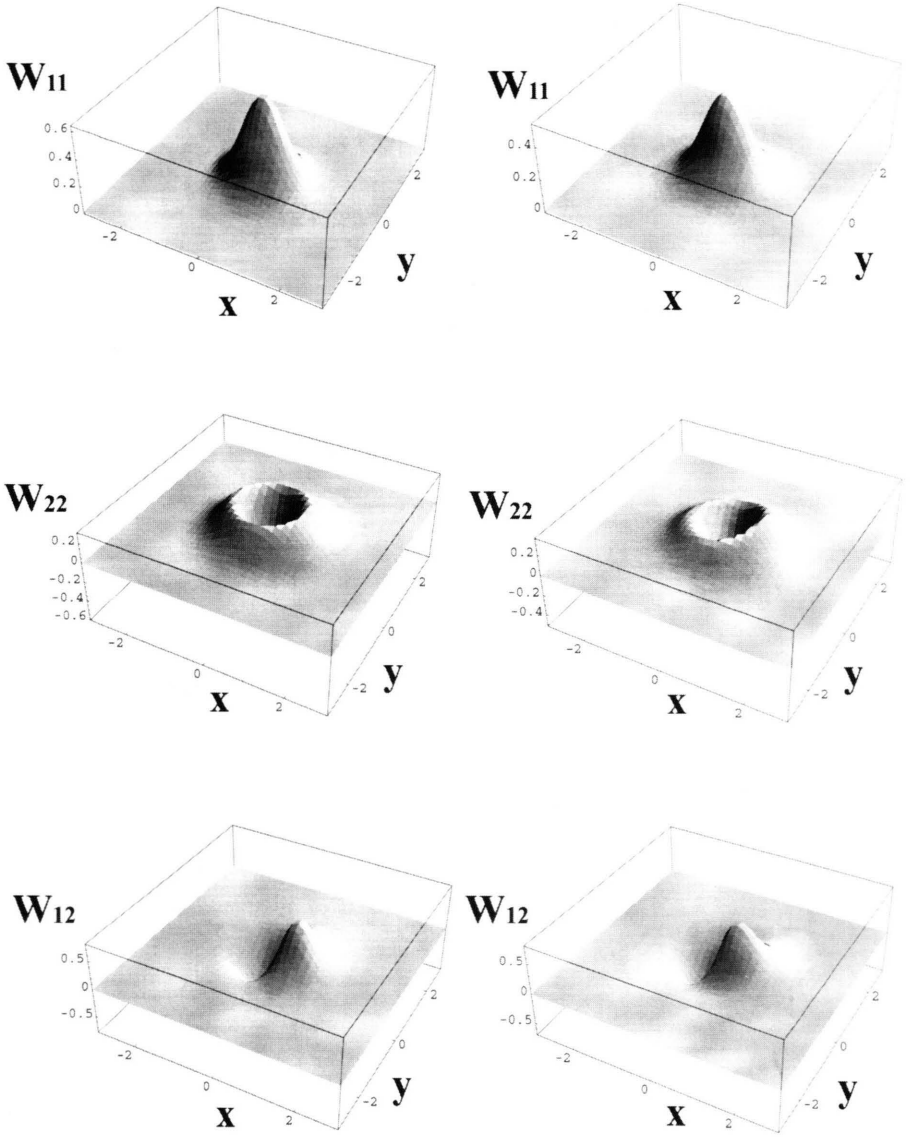

Fig. 1. Simulated tomographic reconstruction of the Wigner functions for the state of (39). Top: $W_{11}(x, y)$; Middle: $W_{22}(x, y)$; Bottom: $W_{12}(x, y)$. Here the ideal distributions are displayed on the left, whereas the reconstructed ones are displayed on the right.

In Fig. 1 we show the numerical reconstruction of the Wigner function corresponding to the state of (39) with $c_1 = c_2 = \sqrt{2}/2$ and $\theta = 0$. The true (i.e. theoretical) distributions are depicted on the left, and the corresponding reconstructed ones on the right. In spite of some differences, the Wigner functions appearing in the matrix (8) are well reconstructed.

In this paper we have proposed a technique suitable to reconstruct the (entangled) state of the cyclotron and spin degrees of freedom of an electron trapped in a Penning trap. It is based on the magnetic bottle configuration, which allows simultaneous measurements of the spin component along the z axis and of the cyclotron excitation number. The cyclotron state is reconstructed with the use of a tomographic-like method, in which the phase of a reference driving field is varied. The application of the present method to several different states [17, 18] confirms that it is quite stable and accurate.

Acknowledgements

This work has been partially supported by INFM (through the 1997 Advanced Research Project "CAT"), by the European Union in the framework of the TMR Network "Microlasers and Cavity QED", and by MURST under the "Cofinanziamento 1997".

[1] E. Schrödinger, Naturwiss. **23**, 807 (1935).
[2] C. H. Bennett, G. Brassard, C. Crepeau, R. Josza, A. Peres, and W. K. Wootters, Phys. Rev. Lett. **70**, 1895 (1993).
[3] D. Bouwmeester, J. Pan, K. Mattle, M. Eibl, H. Weinfurter, and A. Zeilinger, Nature (London) **390**, 575 (1997); D. Boschi, S. Branca, F. De Martini, L. Hardy, and S. Popescu, Phys. Rev. Lett. **80**, 1121 (1998); A. Furusawa, J. L. Sorensen, S. L. Braunstein, C. A. Fuchs, H. J. Kimble, and E. S. Polzik, Science, **282** 706 (1998).
[4] C. H. Bennett and S. J. Wiesner, Phys. Rev. Lett. **69**, 2881 (1992).
[5] A. K. Ekert, Phys. Rev. Lett. **67**, 661 (1991).
[6] See, e. g., the special issue of Proc. Roy. Soc. London Ser. A **454**, 1969 (1998). C. H. Bennett and D. P. DiVincenzo, Nature (London) **404**, 247 (2000).
[7] C. A. Sackett, D. Kielpinski, B. E. King, C. Langer, V. Meyer, C. J. Myatt, M. Rowe, Q. A. Turchette, W. M. Itano, D. J. Wineland, and C. Monroe, Nature (London) **404**, 256 (2000).
[8] L. S. Brown and G. Gabrielse, Rev. Mod. Phys. **58**, 233 (1986).
[9] S. Peil and G. Gabrielse, Phys. Rev. Lett. **83**, 1287 (1999).
[10] M. Freyberger, P. Bardroff, C. Leichtle, G. Schrade, and W. P. Schleich, Physics World **10**, 41 (November 1997).
[11] S. Mancini, A. M. Martins, and P. Tombesi, Phys. Rev. A **61**, 012303 (2000).
[12] S. Mancini and P. Tombesi, Phys. Rev. A **56**, 3060 (1997).
[13] S. Wallentowitz, R. L. de Matos Filho, and W. Vogel, Phys. Rev. A **56**, 1205 (1997).
[14] S. Mancini, P. Tombesi, and V. I. Man'ko, Europhys. Lett. **37**, 79 (1997).
[15] S. Mancini, M. Fortunato, G. M. D'Ariano, and P. Tombesi, J. Opt. Soc. Amer. A **17**, 2529 (2000).
[16] T. Opatrny and D. G. Welsh, Phys. Rev. A **55**, 1462 (1997).
[17] M. Massini, M. Fortunato, S. Mancini, P. Tombesi, and D. Vitali, New Journal of Physics **2**, 20.1 (2000).
[18] M. Massini, M. Fortunato, S. Mancini, and P. Tombesi, Phys. Rev. A (Rapid Communications) **62**, 041401 (2000).